Observations of Binary Population Biofilms

Maarten A. Siebel* and William G. Characklis†
Center for Interfacial Microbial Process Engineering, Montana State University, Bozeman, MT 59717

Received December 4, 1989/Accepted June 4, 1990

Biofilm research has focused on studies of undefined mixed microbial populations and, more recently, on investigations of monopopulation biofilms. In the first case, the biofilm is considered a homogeneous mass, ignoring the properties of individual species. The second case concentrates on the properties and processes of one microbial species in the biofilm. This article describes biofilm experiments conducted with monopopulations of *Klebsiella pneumoniae* and *Pseudomonas aeruginosa* and with binary populations of *K. pneumoniae* and *P. aeruginosa*. Process rates and stoichiometric coefficients were determined for the monopopulation and for the binary population biofilms and evaluated in light of the species distribution in the latter. Results indicate that neither the specific cellular product formation rate nor the glucose–oxygen stoichiometric ratio of *K. pneumoniae* or *P. aeruginosa* in the binary biofilm is affected by the presence of the other species. Consequently, species interaction was not observed. Although the specific cellular growth rate of *K. pneumoniae* is five times that of *P. aeruginosa*, the former species did not dominate the microbial population in the biofilm. Possible reasons for this unexpected behavior are discussed.

INTRODUCTION

A biofilm is an accumulation of microbial cells and inorganic components held together in a polymeric matrix and firmly attached to a substratum. Accumulation of biofilms is encountered in many natural and modulated environments. It may be fundamental to process performance (e.g., fixed-film biological wastewater treatment), or a nuisance resulting in energy losses (fouling), sudden deterioration of water quality (biofilm detachment in water distribution pipelines), and deterioration of substrata (biocorrosion).

Biofilm research has previously focused on undefined, or natural, microbial populations. Because of the heterogeneity of such biofilms, individual properties of the microbial species were not considered. In order to study fundamental processes underlying biofilm accumulation, biofilms of one microbial species (monopopulation biofilms) have also been studied.

This research focused on the accumulation of binary population biofilms, biofilms resulting from the accumulation of two identified microbial species. Processes leading to accumulation and biofilm properties were observed for monopopulation biofilms of *K. pneumoniae* and *P. aeruginosa* and for binary populations of these two species. The objective was to determine if biofilm accumulation of the binary population could be predicted from observation of the monopopulation biofilms.

BACKGROUND

Microbial interactions—the effects organisms in close proximity have on each other—have been investigated for many reasons including biodegradation and algal–bacterial interactions. Biodegradation by consortia of microorganisms includes contributions by several species which are indispensable for the total process.[1] Interactions between algal and bacterial species in suspension have been documented in a variety of environments.[2-6]

Microbial interaction laboratory experiments have generally been conducted in chemostats.[7] In these suspended growth environments, interaction has a strong tendency to result in exclusion of one of the species. In certain cases, mitigating circumstances may result in "balanced coexistence.[8]"

Extrapolation of mixed population results from suspended growth to attached growth conditions is not simple. The homogeneous chemostat environment is quite different from the biofilm system which is characterized by numerous transport processes. Biofilms play a significant role in suspended growth systems. For example, biofilms cause a discrepancy between the mathematical description of a predator–prey relation and observations.[9] Frederickson[7] concludes that "variation of the ratio of chemostat-wetted surface area to culture volume should be an important part of future studies on microbial predator–prey relations."

Most mathematical models of biofilm systems are intended to describe lumped parameters.[10] Models for microbial interactions in biofilms have been reported by a few groups only. Kissel et al.[11] describe a model of a mixed population biofilm system within a completely mixed reactor consisting of an autotroph and a heterotroph as well as an inert particulate fraction. The model allows anoxic conditions to occur but does not consider loss of mass by periodic sloughing or continuous erosion. Consequently, the model cannot describe a biofilm at steady state, but rather one at ever increasing thickness.

* Present address: International Institute for Hydraulic and Environmental Engineering, P.O. Box 3105, 2601 DA DELFT, The Netherlands.
† To whom all correspondence should be addressed.

Biotechnology and Bioengineering, Vol. 37, Pp. 778–789 (1991)

CCC 0006-3592/91/080778-012$04.00

Microbial interaction in a biofilm was theoretically addressed by Wanner and Gujer[10] and illustrated with a heterotrophic–autotrophic biofilm.[12] Under the assumptions that the properties of a biofilm change only in the direction perpendicular to the substratum and that biomass may be treated as a continuum, their model describes a biofilm in terms of (1) changes in the biofilm thickness; (2) dynamics and spatial distribution of the volume fractions of the multiple species where specific growth rates essentially determine the population distribution; and (3) the dynamics and spatial distribution of the concentrations of the multiple substrates. To compensate for the positive biomass production rate, the model includes a velocity of exchange of biomass between the biofilm and the bulk liquid (e.g., biofilm detachment). The model is general in that no particular reactor geometry is employed.

If interorganism distance is a variable of importance in microbial interaction,[13] biofilms seem more likely to result in interaction phenomena than suspended growth. Cell densities per unit biofilm volume are several times those in suspended growth reactors. In addition, biofilm cells have a relatively longer "residence" time near an individual neighbor cell.

MATERIALS AND METHODS

Biofilm Reactor

Biofilm experiments were conducted in a RotoTorque reactor (Fig. 1). The RotoTorque, essentially a Couette vessel,[14,15] consists of two concentric cylinders (polycarbonate), a stationary outer cylinder and a rotating inner cylinder. Twelve removable slides form an integral part of the inside wall of the outer cylinder and permit sampling of the biofilm for the determination of thickness, mass, and biofilm chemical composition.

The bulk liquid is completely mixed by virtue of the cylinder rotation and draft tubes bored through the solid inner cylinder. The draft tubes are positioned at angles so that the rotation of the inner cylinder causes the fluid to rise in the tubes resulting in internal recirculation. By virtue of the complete mixing, the RotoTorque is a Continuous Flow Stirred Tank Reactor (CFSTR). Thus, effluent liquid samples represent the bulk liquid composition. In these experiments, the hydraulic residence time was maintained at 10 minutes so that suspended growth was negligible and all reactor activity could be attributed to the biofilm. Experimental temperature was 21 ±1°C.

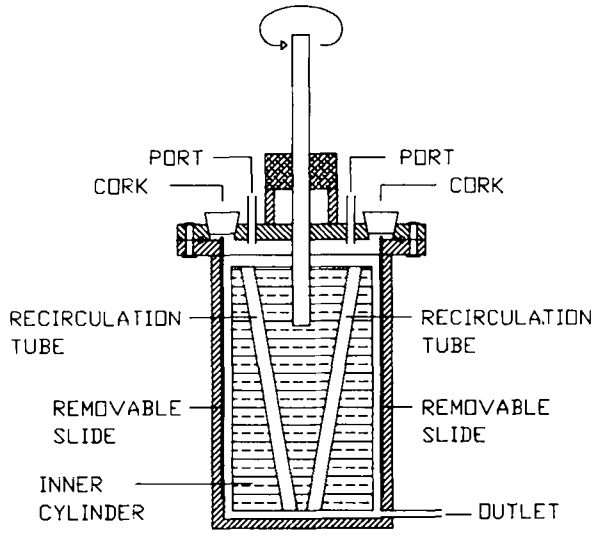

Figure 1. Schematic representation of a RotoTorque reactor.

Material Balance Equations

Material balance equations allow the calculation of biofilm activity, e.g., specific substrate and oxygen uptake rates. Balance equations across the reactor (Table I) were used for substrate [eqs. (1) and (4)], cell [eqs. (2) and (5)] and product carbon [eqs. (3) and (6)] in both the liquid phase and the biofilm. Also, a balance equation was used for liquid phase oxygen [eq. (7)]. For the sake of completeness, liquid-phase activity is included in the balance equations in contrast to equations published previously.[16]

Diffusional resistance to the flux of substrate into the biofilm is taken into account using an effectiveness factor, f_{DS} [eq. (4)], defined as the ratio of the actual flux over the theoretically maximum flux of substrate into the biofilm. A similar term, f_{DO}, can be defined for the flux of oxygen into the biofilm. When, at low substrate concentrations, the flux of substrate is rate-limiting, f_{DS} also relates the specific cellular growth rate in the liquid phase, μ, to the average specific cellular growth rate in the biofilm: $\mu_f = f_{DS}\mu$.

The transfer of oxygen from the gas phase into the (oxygen deficient) reactor liquid is accounted for using a specific mass transfer coefficient, k_c [eq. (7) and Table I]. The value of k_c is determined experimentally using a sterile reactor under standard operating conditions through which a dilution flow, D, of oxygen deficient influent water (oxygen concentration, S_{Oi}) is passed. Oxygen absorption through the reactor wall and pump tubing results in an effluent oxygen concentration, S_{Ol}. Parameter k_c can be calculated according to the following equation:

$$k_c = D\frac{S_{Oi} - S_{Ol}}{S_{Ol} - S_{Os}}$$

where D is the dilution rate (t^{-1}); S_{Oi} is the oxygen concentration in reactor influent ($M_O L^{-3}$); S_{Ol} is the oxygen concentration in reactor effluent ($M_O L^{-3}$); and S_{Os} is the oxygen saturation concentration ($M_O L^{-3}$).

Experimental Procedure

Biofilm experiments were initiated by feeding the clean, autoclaved RotoTorque operating at 200 rpm with a continuous, sterile flow of substrate, calcium,

Table I. Material balance equations across the biofilm reactor (see nomenclature for symbol explanation).

Liquid phase substrate carbon:

$$\frac{dS_{Sl}}{dt} = D(S_{Si} - S_{Sl}) - X_{Mf}\frac{A}{V}r_S - X_{Ml}\left[\frac{\mu}{Y_{MS}} + \frac{r_{Pl}}{Y_{PS}}\right] \quad (1)$$

(net rate of substrate accumulation) = (net rate of substrate inflow) − (rate of substrate uptake by biofilm) − (rate of substrate uptake in liquid phase)

Liquid phase cell carbon:

$$\frac{dX_{Ml}}{dt} = D(X_{Mi} - X_{Ml}) + X_{Mf}\frac{A}{V}r_{Md} + X_{Ml}\mu \quad (2)$$

(net rate of cell mass accumulation) = (net rate of cell mass inflow) + (rate of cell mass detachment) + (rate of cell growth in liquid phase)

Liquid phase product carbon:

$$\frac{dS_{Pl}}{dt} = D(S_{Pi} - S_{Pl}) + S_{Pf}\frac{A}{V}r_{Pd} + X_{Ml}r_{Pl} \quad (3)$$

(net rate of product accumulation) = (net rate of product inflow) + (rate of product detachment) + (rate of product formation in liquid phase)

Biofilm substrate carbon:

$$\frac{dS_S}{dt} = X_{Mf}r_S - X_{Mf}f_{DS}\left[\frac{\mu}{Y_{MS}} + \frac{r_{Pl}}{Y_{PS}}\right] \quad (4)$$

(net rate of substrate accumulation) = (net rate of substrate uptake) − (rate of substrate consumption for cell growth minus product formation)

Biofilm cell carbon:

$$\frac{dX_{Mf}}{dt} = -X_{Mf}r_{Md} + X_{Mf}\mu \quad (5)$$

(net rate of cell mass accumulation) = (net rate of cell mass detachment) + (rate of cellular growth)

Biofilm product carbon:

$$\frac{dS_{Pf}}{dt} = -S_{Pf}r_{Pd} + X_{Mf}r_{Pf} \quad (6)$$

(net rate of product accumulation) = (net rate of product detachment) + (rate of product formation)

Oxygen:

$$\frac{dS_{Ol}}{dt} = (D + k_c)(S_{Os} - S_{Ol}) - X_{Mf}\frac{A}{V}r_O - X_{Ml}\left[\frac{\mu}{Y_{MO}} + \frac{r_{Pl}}{Y_{PO}}\right] \quad (7)$$

(net rate of oxygen accumulation) = (net rate of oxygen inflow in dilution water and through diffusion) − (rate of oxygen uptake by biofilm) − (rate of oxygen uptake for cell growth and product formation in liquid phase)

buffer, and nutrients solutions (Table II). In addition, the reactor is fed with oxygen-saturated, sterile dilution water at $D \geq \mu_m$.

Inoculation (experimental time of 0 h) of the clean RotoTorque was accomplished by feeding the reactor for 12 h with a suspended population from a chemostat (for the binary population biofilm experiments, the reactor was inoculated with the bacterial suspensions from two chemostats). The chemostat was operated at steady-state conditions at a dilution rate of 0.3 h^{-1}. The inlet substrate concentration to the chemostat was 40 g glucose carbon m^{-3}, the steady-state cell density was 10^{12}–10^{14} cells m^{-3}. Cells adsorbed to the Rototorque substratum during the period of inoculation leading to the accumulation of the biofilm as the experiment progressed.

Analytical Procedure

Samples were collected at regular intervals from the RotoTorque effluent for determination of cell carbon, product carbon, glucose carbon, and dissolved oxygen. Biofilm samples were analyzed for cell carbon and product carbon according to Bakke et al.[16] In addition, wet biofilm thickness was measured as described by

Table II. Composition of nutrient solution.

	Chemostat	RotoTorque	Units
Glucose-carbon	40.0	8.0	g m^{-3}
NH_4CL	36.0	7.2	g m^{-3}
$MgSO_4 \cdot 7H_2O$	10.0	2.0	g m^{-3}
$(NH_4)6Mo_7O_{24} \cdot 4H_2O$	0.005	0.001	g m^{-3}
$ZnSO_4 \cdot 7H_2O$	0.5	0.1	g m^{-3}
$MnSO_4 \cdot H_2O$	0.040	0.008	g m^{-3}
$CuSO_4 \cdot 5H_2O$	0.010	0.002	g m^{-3}
$Na_2B_4O_7 \cdot 10H_2O$	0.005	0.001	g m^{-3}
$FeSO_4 \cdot 7H_2O$	0.560	0.112	g m^{-3}
$(HOCOCH_2)_3N$	2.0	0.4	g m^{-3}
$CaCO_3$-Ca	—	25.0	g m^{-3}
Na_2HPO_4	568.0	213.0	g m^{-3}
KH_2PO_4	544.0	204.0	g m^{-3}
Final pH	6.8	6.8	dimensionless

Bakke and Ollsen.[17] Air dried biofilm samples were used for Nomarski microscopy.

Cells per unit volume or unit surface area were counted in homogenized effluent samples and in the resuspended, homogenized biofilm samples of monopopulation biofilms using both epifluorescence microscopy and plates. Epifluorescence microscopy coupled to image analysis allowed the determination of the cell size. Cell numbers combined with cell size were converted to cell carbon.[16] Differential plating of homogenized effluent samples and of resuspended, homogenized biofilm samples allowed determination of cell numbers of each species in the binary population. Conversion of cell numbers to cell mass allowed the calculation of the relative mass fractions of the two species in the binary population biofilms. Some characteristics of the two microbial species are listed in Table III. Progressions for biofilm accumulation were fitted with the logistic equation.[25]

RESULTS

Biofilm experiments included three sets of four experiments each, the first set was conducted with *K. pneumoniae* and the second set with *P. aeruginosa,* both as monopopulations. The third set of experiments was conducted with both organisms in a binary population. The variable in these experiments was the microbial inoculum. Otherwise, conditions were the same in all experiments except for the influent substrate concentration (S_{Si} was 20 g carbon m^{-3} for two binary population experiments and 10 g carbon m^{-3} for all other (10) experiments). Biofilm accumulation, progression of biofilm thickness, biofilm species distribution, the specific product formation rate, and the glucose–oxygen stoichiometric ratio are compared for biofilms of *K. pneumoniae, P. aeruginosa,* and for the binary population.

Biofilm Accumulation

Monopopulation biofilms of *K. pneumoniae* and *P. aeruginosa* differ in the initial colonization stage and in subsequent biofilm accumulation. Similarly, accumulation of the binary population biofilm is different from that observed by the monopopulation biofilms. Nomarsky interference micrographs (Figs. 2, 3, and 4) illustrate the dried biofilm surface at various experimental times.

K. pneumoniae accumulates in small, "patchy" clusters of cells [Fig. 2(a)] which expand rapidly. Cells aggregate and grow enlarging the clusters parallel and perpendicular to the substratum resulting in the formation of "microtowers" [Fig. 2(b)] which can reach a height of 60 μm or more with bare substratum between the towers. *P. aeruginosa* colonizes the substratum in a relatively uniform distribution [Fig. 3(a)]. Cells grow and multiply, reducing intercellular distance and gradu-

Table III. Relevant characteristics of *K. pneumoniae* and *P. aeruginosa.*

	K. pneumoniae	Reference	*P. aeruginosa*	Reference
Shape	rod shaped	18	rod shaped	18
Breadth (μm)	0.3–1.5	18	0.5–0.8	18
Length (μm)	0.6–6.0	18	1.5–4.0	18
EPS formation	yes		yes	
EPS composition	glucose, fucose, glucuronic acid, and pyruvic acid	19	primarily mannuronic and guluronic acid	23
Motility	nonmotile		polar flagella	18
Modes of	facultative		obligate aerobe	
Respiration	anaerobic	20	except when	
Denitrification	yes	20	nitrate present	20
Metabolism	chemoorganotroph	21	chemoorganotroph	
Gram stain	negative	18	negative	18
Optimal temperature	35–37°C	18	35–37°C	20
Optimal pH	7.2	18	6.8	20
Maximum specific Growth rate (h^{-1})	2.0	22	0.4	24
Half saturation Concentration (g C m^{-3})	1.4	22	2.0	22

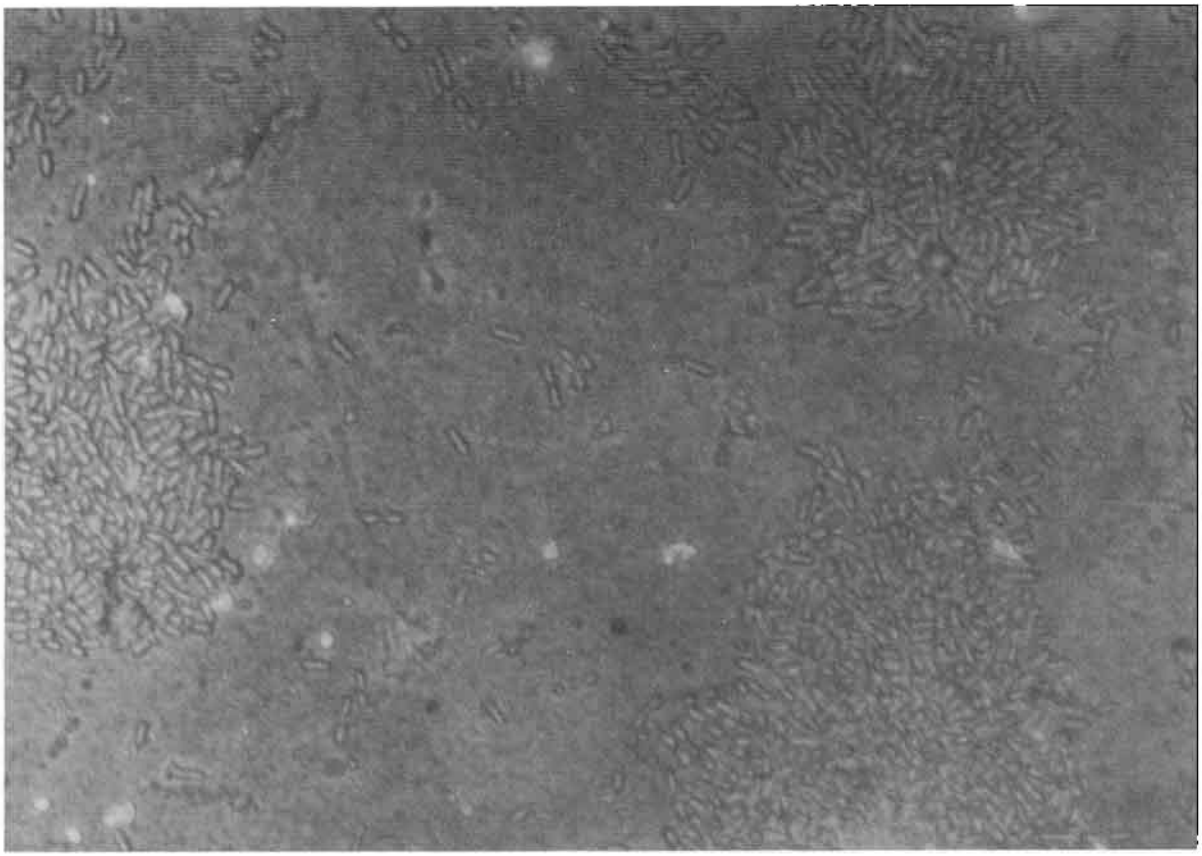

(a)

(b)

Figure 2. Accumulation of *K. pneumoniae* on polycarbonate substratum (Nomarsky microscopic picture) taken (a) 50 h after inoculation (magnification of 625×) and (b) 100 h after inoculation (magnification of 500×). Cell clusters expand but uncolonized space between clusters remains.

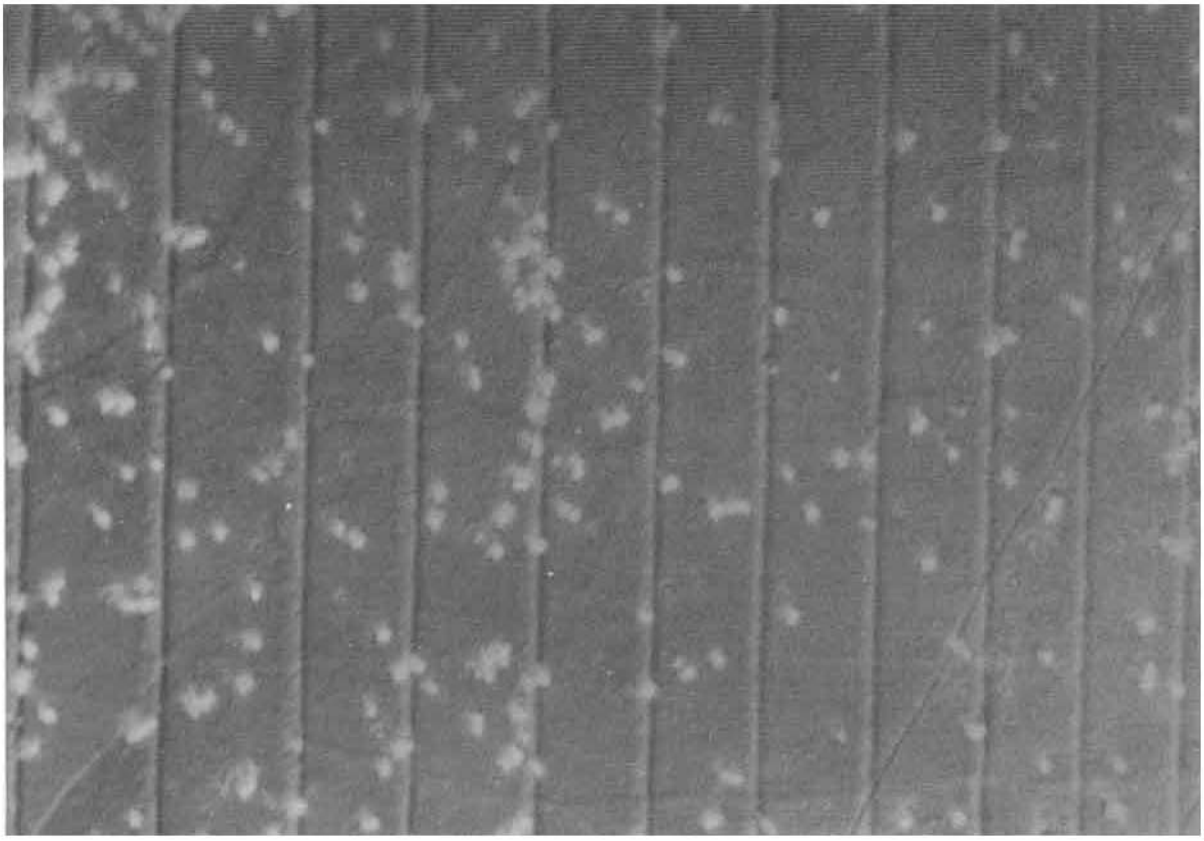

(a)

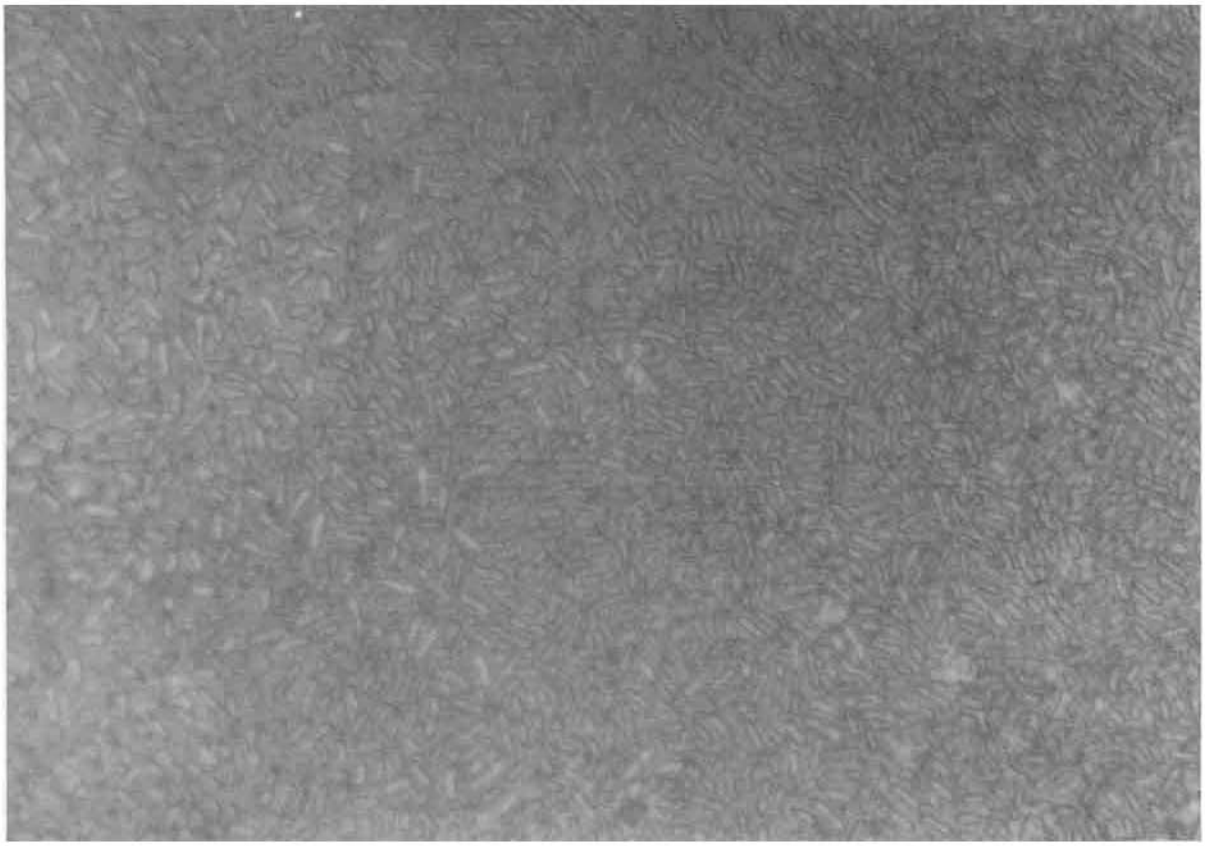

(b)

Figure 3. Accumulation of *P. aeruginosa* on polycarbonate substratum (Nomarsky microscopic picture) taken (a) 50 h after inoculation (magnification of 625×) and (b) 65 h after inoculation (magnification of 625×). A monolayer of closely packed cells is shown.

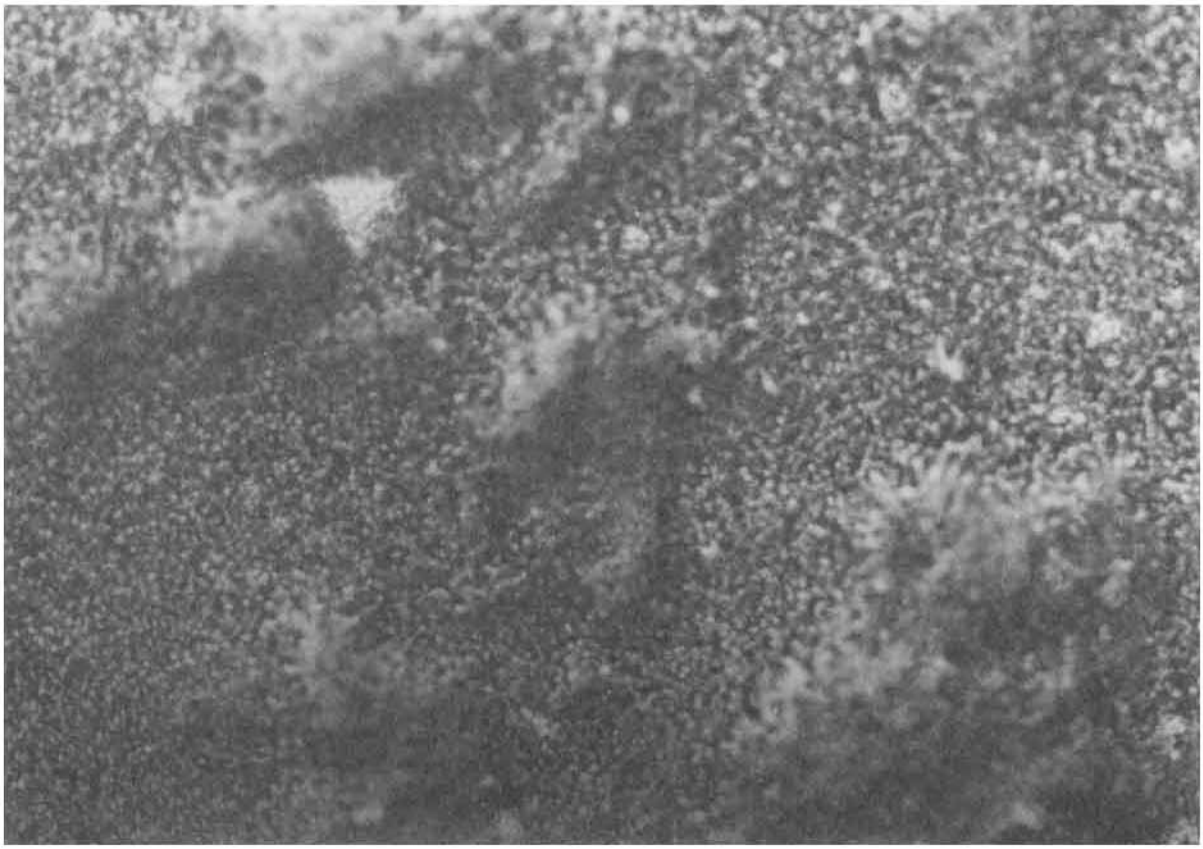

(a)

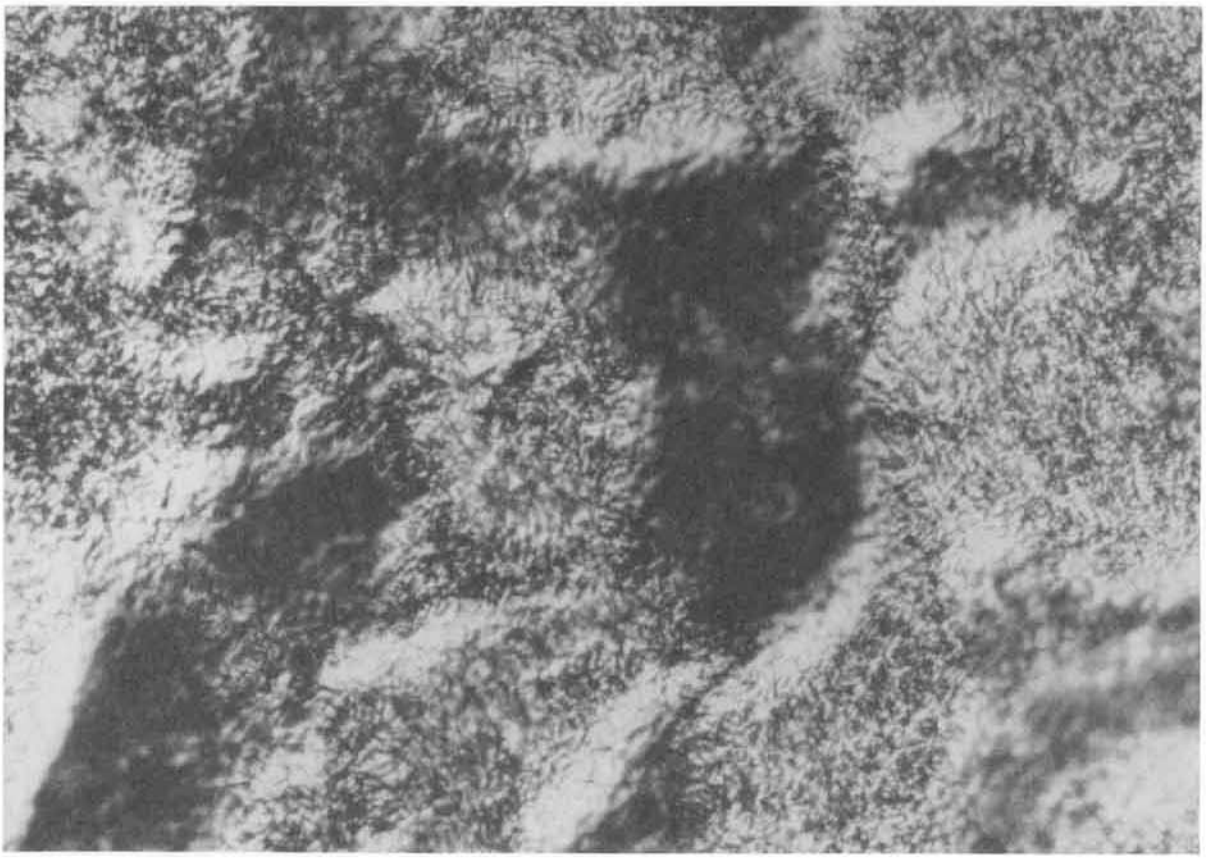

(b)

Figure 4. Accumulation of a binary population biofilm on polycarbonate substratum (Nomarsky microscopy) taken (a) 123 h after inoculation (magnification of 500×) and (b) 208 h after inoculation (magnification of 500×). Surface roughness increases when binary population biofilms get older.

ally forming a smooth biofilm [Fig. 3(b)]. A binary population biofilm forms a relatively smooth film with peaks extending above the smooth film surface [Fig. 4(a)]. Gradually, surface roughness increases [Fig. 4(b)].

Biofilm Thickness

The progression of biofilm thickness can be compared in terms of the means and the standard deviations of the measurements. The mean thickness for *K. pneumoniae* at the end of the experimental run was approximately 15 μm while the standard deviation was approximately 35 μm [Fig. 5(a)]. Even after 190 h, some measurements indicate zero biofilm thickness although biofilm was detected as early as 25 h into the experiment.

P. aeruginosa biofilm thickness was not measurable in the first 50 h of the experiment but the biofilm accumulated rapidly thereafter [Fig. 5(b)]. Mean *P. aeruginosa* biofilm thickness is approximately twice that of *K. pneumoniae,* while the standard deviation is considerably smaller (20%) than that for *K. pneumoniae.* Consequently, a *P. aeruginosa* biofilm is smooth as compared to that of *K. pneumoniae.* Accumulation of the binary population biofilm is visible only after over 100 h into the experiment. The mean of the thickness measurements for the 10 g carbon m^{-3} experiments, was approximately 40 μm, the standard deviation was 10 μm [Fig. 5(c)]. Biofilm thickness approximately doubled for the 20 g carbon m^{-3} experiments (not shown).

Biofilm Species Distribution

The relative concentration of *K. pneumoniae* and *P. aeruginosa* was determined for the binary population biofilm. Progression of the means and the means plus or minus the standard deviation of the *K. pneumoniae* cell mass fraction was described using the logistic equation.[25] Figure 6 shows the progression of the biofilm cell mass fraction occupied by *K. pneumoniae* (area below the "means" line) and by *P. aeruginosa* (area above the "means" line) for both the 10 and the 20 g glucose carbon m^{-3} experiments. The contribution of the *K. pneumoniae* biofilm cell mass fraction, initially approximately 50%, decreased to approximately 26% after 150 h. Moreover, the standard deviation of the mass fraction measurements decreased from approximately 15% initially, to approximately 7% after 150 h.

Biofilm Specific Product Formation Rate

The biofilm specific product formation rate (r_{Pf}) is the rate at which product is being formed on a unit cell mass basis. r_{Pf} can be determined by rearranging eq. (6) (Table I):

$$r_{Pf} = \frac{S_{Pf}}{X_{Mf}} r_{Pd} + \frac{1}{X_{Mf}} \frac{dS_{Pf}}{dt} \tag{8}$$

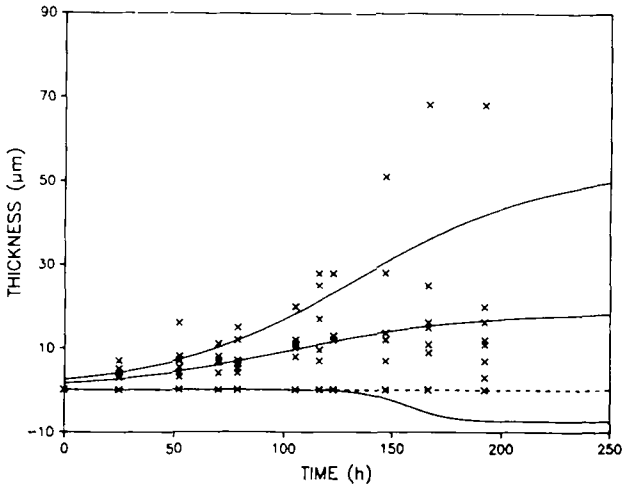

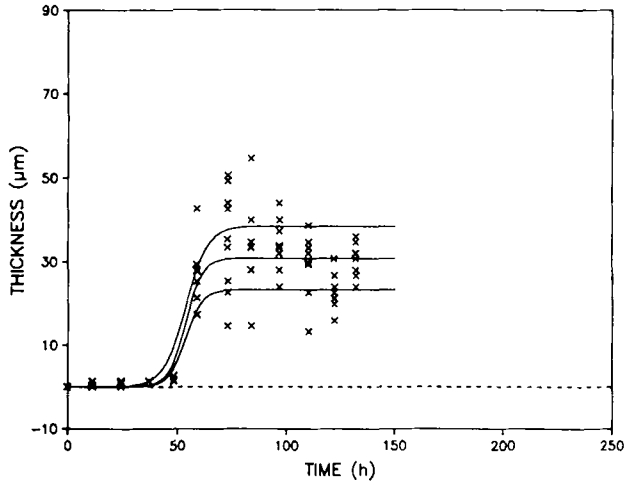

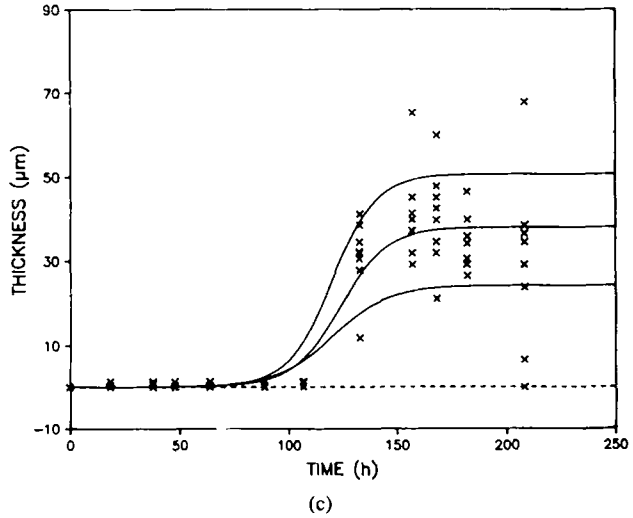

Figure 5. Progression of biofilm thickness for (a) *K. pneumoniae,* (b) *P. aeruginosa,* and (c) the binary population. Lines represent time smoothed means (middle line in each graph), means plus the standard deviation of the means (top line) and means minus the standard deviation of the means (bottom line).

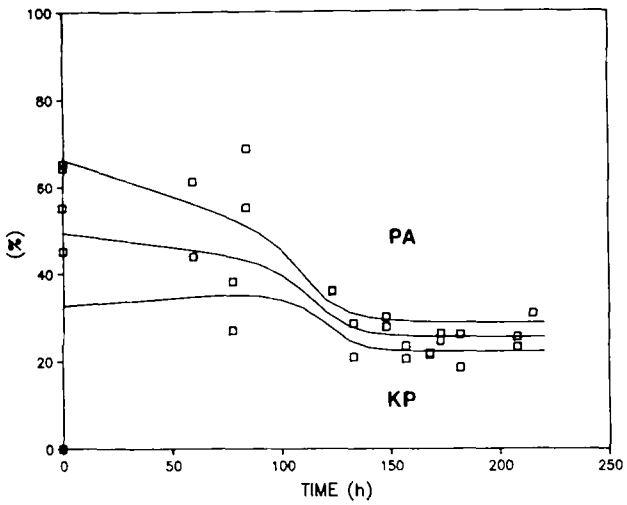

Figure 6. Progression of biofilm cell mass fraction for the binary population biofilms. Lines represent time smoothed means (middle line), means plus the standard deviation of the means (top line) and means minus the standard deviation of the means (bottom line): (KP) *K. pneumoniae*, (PA) *P. aeruginosa*.

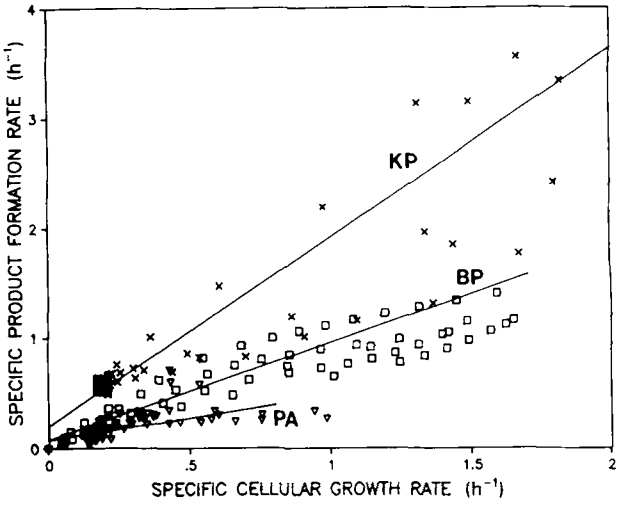

Figure 7. Comparison of data points and kinetic models for the product formation kinetics for monopopulation biofilms of *K. pneumoniae* and *P. aeruginosa* and for binary population biofilms. See Table IV for statistical information about the regression lines: (KP) *K. pneumoniae*, (PA) *P. aeruginosa*, and (BP) Binary Population.

where r_{Pf} is the specific rate of product formation in biofilm ($M_P M_M^{-1} t^{-1}$); S_{Pf} is the product carbon concentration in biofilm ($M_P L^{-2}$); X_{Mf} is the cell carbon concentration in biofilm ($M_M L^{-2}$); r_{Pd} is the specific rate of product detachment (t^{-1}); and t is the time (t). Moreover, dividing the mass balance of biofilm cell carbon [eq. (5) Table I] by X_{Mf} and substituting μ_f for $f_{DS}\mu$,

$$\frac{1}{X_{mf}} \frac{dX_{Mf}}{dt} = -r_{Md} + \mu_f \tag{9}$$

permits the calculation of the average biofilm specific cellular growth rate, μ_f. The biofilm specific product formation rate is a linear function of biofilm specific cellular growth rate [eq. (10)] with a growth-associated and a non-growth-associated component[26]:

$$r_{Pf} = k_{Pg} \cdot \mu_f + k_{Pn} \tag{10}$$

where k_{Pg} is the growth-associated product formation coefficient ($M_P M_M^{-1}$); k_{Pn} is the non-growth-associated product formation rate coefficient ($M_P M_M^{-1} t^{-1}$); and μ_f is the average specific cellular growth rate in biofilm (t^{-1}). Linear regression of r_{Pf} vs. μ_f for the biofilm experiments (Fig. 7) results in values for k_{Pg} and k_{Pn} (Table IV).

Biofilm Glucose–Oxygen Stoichiometric Ratio

The biofilm glucose–oxygen stoichiometric ratio (η_{SO}) is the ratio of the specific rate of glucose consumption in the biofilm (r_S) to the specific rate of oxygen consumption in the biofilm (r_O).

$$\eta_{SO} = \frac{r_S}{r_O} \tag{11}$$

The biofilm specific glucose consumption rate can be determined by rearranging eq. (1) (Table I) and assuming that the suspended cellular activity is negligible ($X_{Ml} = 0$):

$$r_S = \frac{D(S_{Si} - S_{Sl}) - \dfrac{dS_{Sl}}{dt}}{X_{Mf} \dfrac{A}{V}} \tag{12}$$

Similarly, the biofilm specific oxygen consumption rate can be evaluated by rearranging eq. (7) (Table I) and assuming that the suspended cellular activity is negligible ($X_{Ml} = 0$:

$$r_O = \frac{(D + k_c)(S_{Os} - S_{Ol}) - \dfrac{dS_{Ol}}{dt}}{X_{Mf} \dfrac{A}{V}} \tag{13}$$

Table IV. Specific growth- and non-growth-associated product formation coefficients in the biofilm for *K. pneumoniae*, *P. aeruginosa*, and the binary population (values for k_{Pg} and k_{Pn} are given as means plus or minus the standard deviation). See also Figure 7.

	K. pneumoniae	*P. aeruginosa*	Binary population
k_{Pg} (g g^{-1})	1.72 ±0.11	0.36 ±0.07	0.75 ±0.03
k_{Pn} (g g^{-1} h^{-1})	0.20 ±0.04[a]	0.10 ±0.07[a]	0.08 ±0.02[a]
R^2 (dimensionless)	0.74	0.31	0.90

[a] Values for k_{Pn} are different from zero at the 5% level of significance.

The specific glucose consumption rate is essentially a linear function of the specific oxygen consumption rate (Fig. 8) for the biofilm experiments with *K. pneumoniae, P. aeruginosa,* and the binary population. A statistical summary of the linear regressions is presented in Table V.

DISCUSSION

The objective of this research was to describe accumulation of a binary population biofilm of *K. pneumoniae* and *P. aeruginosa* in terms of the accumulation of the monopopulation biofilms of *K. pneumoniae* and *P. aeruginosa.* Values for two biofilm parameters, the biofilm specific product formation rate, including the biofilm specific growth- and non-growth-associated product formation coefficient, and the biofilm glucose–oxygen stoichiometric ratio, were determined in the monopopulation biofilms and in the binary population biofilms.

When assuming no interaction between species, the biofilm specific growth-associated product formation coefficient and the biofilm glucose–oxygen stoichiometric ratio can also be predicted on the basis of the species distribution. By adding the products of the growth-associated product formation coefficient for each species in the monopopulation and the cell mass fraction of the species in the binary population, a growth-associated product formation coefficient is found of 0.72 ±0.11 g product carbon (g cell carbon)$^{-1}$. At the 5% level of significance, this calculated value is not different from the one determined experimentally, i.e., 0.75 ±0.03 g product carbon (g cell carbon)$^{-1}$ (Table IV). Similarly, by adding the products of the glucose–oxygen stoichiometric ratio for each species in the monopopulation and the cell mass fraction of the species in the binary population, a glucose–oxygen stoichiometric ratio is found of 1.47 ±0.20 g product carbon (g cell carbon)$^{-1}$. At the 5% level of significance, this calculated value is not different from the one determined experimentally, i.e., 1.46 ±0.04 g glucose carbon consumed (g oxygen consumed)$^{-1}$ (Table V). Therefore, *K. pneumoniae* or *P. aeruginosa* in the binary population biofilm is not affected by the presence of the other organism.

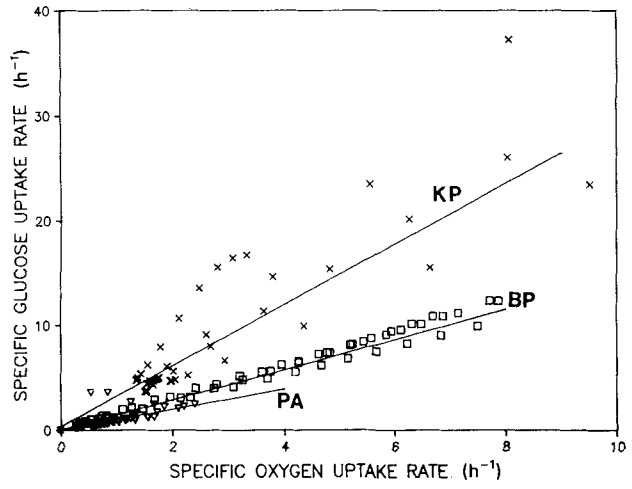

Figure 8. Comparison of data points and kinetic models for the glucose–oxygen stoichiometric ratio for monopopulation biofilms of *K. pneumoniae* and *P. aeruginosa* and for binary population biofilms. See Table V for statistical information about the regression lines: (KP) *K. pneumoniae;* (PA) *P. aeruginosa;* and (BP) Binary Population.

Accumulation of the binary population biofilm may also be described in terms of morphology. *K. pneumoniae* accumulates in clusters with bare substratum between the clusters (Fig. 2). In contrast, *P. aeruginosa* accumulates as a relatively smooth film (Fig. 3). The binary population biofilm appears to consist of clusters which extend above a smooth base film (Fig. 6). Considering the morphology of the monopopulation biofilms and remembering that species interaction in the binary population was not detected, we speculate that the base film consists of *P. aeruginosa* while *K. pneumoniae* forms the clusters. Techniques for the nondestructive identification of biofilm species were not available. Hence this concept could not be proven.

Interaction between the species does not appear to play an important role in the microbial mass distribution considering the fact that at steady-state conditions, both species are present in significant mass concentrations (Fig. 6). This may seem inconsistent with the observed difference in growth kinetics: the maximum specific cellular growth rate, μ_m, of *K. pneumoniae* is five times the value for μ_m of *P. aeruginosa.* As a result, *P. aeruginosa* could be outcompeted by *K. pneumoniae.* However, various species specific phenomena may help explain the observations.

K. pneumoniae has a high specific rate of product formation. Moreover, this species is nonmotile with cells aggregating at the substratum and forming clusters or 'trapped' cells.[27] Furthermore, when calculating the effectiveness factor for the flux of substrate into a biofilm (as a function of the biofilm thickness, substrate concen-

Table V. Glucose–oxygen stoichiometric ratio (η_{SO}) in the biofilm for *K. pneumoniae, P. aeruginosa,* and the binary population (values for η_{SO} and I are given as means plus or minus the standard deviation). See also Figure 8. I is the intercept of the lines.

	K. pneumoniae	*P. aeruginosa*	Binary population
η_{SO} (g g^{-1})	2.90 ±0.08	0.96 ±0.18	1.46 ±0.04
I (g g^{-1} h^{-1})	0.33 ±0.37[a]	0.07 ±0.20[a]	0.19 ±0.13[a]
R^2 (dimensionless)	0.93	0.34	0.94

[a] The intercepts (I) are different from zero at the 5% level of significance.

tration, biofilm cell carbon density, effective diffusion coefficient within the microbial mass, yield of cell mass from substrate mass, yield of product mass from substrate mass, growth- and non-growth-associated production formation coefficients and maximum specific cellular growth rates[28]), the substrate diffusion resistance is three times higher for *K. pneumoniae* than for a comparably smooth *P. aeruginosa* biofilm of 30-μm thickness.[22] Thus, only the outside layer of cells in a cluster of *K. pneumoniae* has a growth rate determined by the bulk liquid substrate concentration, while the growth rate of cells in the core of the cluster is considerably less. This could lower the volume average specific cellular growth rate of a *K. pneumoniae* biofilm considerably. In contrast, diffusional resistance of a *P. aeruginosa* biofilm is relatively small[16,24] and the average specific biofilm cellular growth rate is determined by the bulk liquid substrate concentration.

Population dynamics in biofilms are important to modulating biofilm accumulation and activity. The experimental observations suggest that factors other than specific growth rate (e.g., colonial morphology) may significantly influence spatial distribution of cells and relative cell numbers in biofilms.

CONCLUSIONS

The following conclusions can be drawn from experiments with *K. pneumoniae* and *P. aeruginosa* in biofilms for the range of experimental conditions tested:

1. There is no apparent interaction between *K. pneumoniae* or *P. aeruginosa* in a binary population biofilm.
2. Specific product formation rate of *K. pneumoniae* or *P. aeruginosa* in the binary population biofilm is not affected by the presence of the other species.
3. Glucose–oxygen stoichiometric ratio of *K. pneumoniae* or *P. aeruginosa* in the binary population biofilm is not affected by the presence of the other species.
4. *K. pneumoniae* and *P. aeruginosa* are present in the biofilm in approximately equal mass concentrations although the maximum specific cellular growth rate of *K. pneumoniae* is five times the maximum specific cellular growth rate of *P. aeruginosa.*

Financial support is acknowledged from the Office of Naval Research (No. 290423), the National Science Foundation (No. 290507), Montana State University Engineering Experiment Station (No. 162000) and the I.P.A. Associates Program. Gerrie Siebel is gratefully acknowledged for the artwork.

NOMENCLATURE

A	substratum area (L^2)
D	dilution rate (= flow rate F of dilution water into reactor divided by volume of reactor) (t^{-1})
f_{DS}	effectiveness factor for substrate diffusion (dimensionless)
f_{DO}	effectiveness factor for substrate diffusion (dimensionless)
F	flow rate of dilution water ($L^3\,t^{-1}$)
k_c	specific mass transfer coefficient for dissolved oxygen (t^{-1})
k_{Pg}	a growth-associated product formation coefficient ($M_P\,M_M^{-1}$)
k_{Pn}	a non-growth-associated product formation rate coefficient ($M_P\,M_M^{-1}\,t^{-1}$)
N_O	flux of dissolved oxygen into reactor system ($M_O\,L^{-2}\,t$)
r_{Md}	specific cell detachment rate (t^{-1})
r_{Pd}	specific product detachment rate (t^{-1})
r_{Pf}	specific product formation rate in biofilm ($M_P\,M_M^{-1}\,t^{-1}$)
r_{Pl}	specific product formation rate in liquid phase ($M_P\,M_M^{-1}\,t^{-1}$)
r_O	biofilm specific oxygen consumption rate ($M_O\,M_M^{-1}\,t^{-1}$)
r_S	biofilm specific substrate consumption rate ($M_S\,M_M^{-1}\,t^{-1}$)
S_{Ol}	concentration of oxygen in liquid phase ($M_O\,L^{-3}$)
S_{Os}	oxygen saturation concentration in influent ($M_O\,L^{-3}$)
S_{Pf}	product carbon concentration in biofilm ($M_P\,L^{-2}$)
S_{Pi}	product carbon concentration in influent ($M_P\,L^{-3}$)
S_{Pl}	product carbon concentration in liquid phase ($M_P\,L^{-3}$)
S_{Sf}	substrate carbon concentration in biofilm ($M_S\,L^{-3}$)
S_{Si}	substrate carbon concentration in influent ($M_S\,L^{-3}$)
S_{Sl}	substrate carbon concentration in liquid phase ($M_S\,L^{-3}$)
t	time (t)
V	reactor volume (L^3)
X_{Mf}	cell carbon concentration in biofilm ($M_M\,L^{-2}$)
X_{Mi}	cell carbon concentration in influent ($M_M\,L^{-3}$)
X_{Ml}	cell carbon concentration in liquid phase ($M_M\,L^{-3}$)
Y_{MO}	yield of cell carbon from oxygen ($M_M\,M_O^{-1}$)
Y_{MS}	yield of cell carbon from substrate carbon ($M_M\,M_S^{-1}$)
Y_{PO}	yield of product carbon from oxygen ($M_P\,M_O^{-1}$)
Y_{PS}	yield of product carbon from substrate carbon ($M_P\,M_O^{-1}$)
μ	specific cellular growth rate in liquid phase (t^{-1})
μ_f	average specific cellular growth rate in biofilm (t^{-1})
μ_m	maximum specific cellular growth rate (t^{-1})
η_{SO}	biofilm glucose–oxygen stoichiometric ratio ($M_S\,M_O^{-1}$)

References

1. J. H. Slater and D. Lovatt, in *Microbial degradation of organic compounds,* Gibson, Ed. (Wiley, New York, 1984), p. 439.
2. A. Escher and W. G. Characklis, *Biotechnol. Bioeng.,* **24,** 2283 (1982).
3. T. K. Haack and G. A. McFeters, *Microb. Ecol.,* **8,** 115 (1982).
4. P. E. Holmes, *Appl. Environ. Microbiol.,* **Dec.,** 1391 (1982).
5. K. A. Sandbeck and D. M. Ward, *Appl. Environ. Microbiol.,* **41,** 775 (1981).
6. G. E. Schiefer and D. E. Caldwell, *Appl. Environ. Microbiol.,* **44,** 84 (1982).
7. A. G. Frederickson, *Ann. Rev. Microbiol.,* **31,** 63 (1977).
8. H. VanGemerden, *Microbial Ecol.,* **1,** 104 (1974).
9. H. H. Topiwala and G. Hamer, *Biotechnol. Bioeng.,* **13,** 919 (1971).
10. O. Wanner and W. Gujer, *Biotechnol. Bioeng.,* **28,** 314 (1986).
11. J. C. Kissel, P. L. McCarthy, and R. L. Street, *J. Environ. Eng.,* **110** (2), 393 (1984).
12. O. Wanner and W. Gujer, *Water Sci. Technol.,* **17,** 27 (1985).
13. D. J. Crisp, in *Marine biodeterioration: an interdisciplinary study,* Costlow and Tipper, Eds. (Naval Institute Press, Annapolis, MD, 1981), p. 103.
14. G. I. Taylor, *Proc. Roy. Soc. Lond.,* **A157,** 546 (1936).
15. A. K. Wang and L. W. Gelhar, *J. Fluids Eng.* **96,** 265 (1974).
16. R. Bakke, M. G. Trulear, J. A. Robinson, and W. G. Characklis, *Biotechnol. Bioeng.,* **26,** 1418 (1984).
17. R. Bakke and P. Q. Ollsen, *J. Microb. Met.* **5,** 1 (1986).
18. H. G. Holt (Williams & Wilkins Co. Baltimore, MD, 1977).
19. C. Erbing, L. Kenne, B. Lindberg, and J. Lönngren, *Carbohydr. Res.,* **50,** 115 (1976).
20. R. E. Buchanan and N. E. Gibbons, Eds. (Williams and Wilkins Co., Baltimore, MD, 1974).

21. I. Sutherland, in *Surface carbohydrates of the prokaryotic cell,* Sutherland, Ed., (Academic, London, 1977), p. 27.
22. M. A. Siebel, Ph.D. dissertation, Montana State University, Bozeman, MT, 1987.
23. F. A. Mian, T. R. Jarman, and R. C. Righelato, *J. Bacteriol.,* **134,** 418 (1978).
24. M. G. Trulear, Ph.D. dissertation, Montana State University, Bozeman, MT, 1983.
25. W. H. Kirchhoff (Chemical Thermodynamics Division Center for Chemical Physics, National Bureau of Standards, Gaithersburg, MD 20899, 1986).
26. R. Luedeking and E. L. Piret, *J. Biochem. Microbiol. Technol. Eng.,* **1**(4), 393 (1959).
27. J.W. Costerton, T. J. Marrie, and K.-J. Cheng, in *Bacterial adhesion,* D. C. Savage, and M. Fletcher, Eds. (Plenum, New York, 1975), p. 3.
28. B. Atkinson and I. J. Davies, *Trans. Inst. Chem. Eng.,* **52,** 248 (1974).